

PROGRESS REPORT ON THE INFLUENCE OF TEST TEMPERATURE AND GRAIN BOUNDARY CHEMISTRY ON THE FRACTURE BEHAVIOR OF ITER COPPER ALLOYS
– M. Li, J. F. Stubbins (University of Illinois), D. J. Edwards (Pacific Northwest National Laboratory)

OBJECTIVE

The objective of this study is to determine the effects of temperature, changes in grain boundary chemistry and changes in other microstructural features on the tensile and fracture behavior of GlidCop™ CuAl25, Hycon 3HP CuNiBe, and Elbrodur CuCrZr at elevated temperatures.

SUMMARY

This collaborative study was initiated to determine mechanical properties at elevated temperatures of various copper alloys by University of Illinois and Pacific Northwestern National Lab (PNNL) with support of OMG Americas, Inc. and Brush Wellman, Inc. This report includes current experimental results on notch tensile tests and pre-cracked bend bar tests on these materials at room temperature, 200 and 300°C. The elevated temperature tests were performed in vacuum and indicate that a decrease in fracture resistance with increasing temperature, as seen in previous investigations. While the causes for the decreases in fracture resistance are still not clear, the current results indicate that environmental effects are likely less important in the process than formerly assumed.

PROGRESS AND STATUS

1. Introduction

High strength, high conductivity copper alloys have been considered as candidate materials for first wall and divertor heat sink applications in the proposed International Thermonuclear Experimental Reactor (ITER) [1]. Three different copper alloys are under consideration, namely dispersion-strengthened CuAl25 alloy, and precipitation-hardened CuNiBe and CuCrZr alloys. This study focuses on the following copper alloys: GlidCop™ CuAl25, Hycon 3HP CuNiBe, and Elbrodur CuCrZr. Although the processing and microstructures of these three alloys are quite different, the general trend for each alloy is that the tensile properties and fracture toughness decrease as temperature increases, and in the case of the CuAl25 and CuNiBe, the fracture toughness drops very rapidly at $T \geq 200^\circ\text{C}$ [2]. The toughness degradation with increasing temperature has been presumed to be related to an environmental effect and/or an impurity effect. However, no evidence supports the idea that the environmental effect is the only factor responsible for the poor toughness. Vacuum tests still showed that the fracture toughness of CuAl25, CuNiBe decreases with increasing temperature. This study focused on the effects of temperature and grain boundary chemistry change on fracture behaviors of three copper alloys.

2. Experimental Procedures

Three copper alloys, GlidCop™ CuAl25, Hycon 3HP CuNiBe, and Elbrodur CuCrZr were tested at room temperature, 200 and 300°C, and analyzed by optical microscopy, scanning electron microscopy, and Auger electron microscopy.

The GlidCop™ CuAl25 (Heat #C-8064, ITER grade 0) was supplied by OMG Americas, Inc. in the form of 1 inch thick plate with a pure copper cladding. It was in the cross-rolled and annealed condition, and boron deoxidized. The grain size is about 4 μm in width and 15 μm in length [3]. The Hycon 3HP CuNiBe (Heat #46546) was supplied by Brush Wellman, Inc. in the form of 1.25 inch thick plate. The plates were in the HT temper condition (cold worked and aged), and then heat-treated again to produce an AT tempered condition (solutionized, quenched, and aged). It has equiaxed grains of about 40 μm [3]. The Elbrodur CuCrZr (Heat # AN4946) was supplied by S. J. Zinkle in the cold worked and aged condition (F37 temper). This copper alloy has grains 25 μm in width and 48 μm in length [3]. The chemical compositions of the three copper alloys are listed in Table 1.

Table 1 Chemical Composition (wt%) of three copper alloys

Materials	Chemical Composition (wt%)				
GlidCop™ CuAl25	0.25 Al	23ppm Fe	6ppm Pb	~250ppm B	10ppm S
Hycon 3HP CuNiBe	0.35 Be	1.92 Ni	<0.01 Co	<0.01 Fe	<0.03 Cr
Elbrodur CuCrZr	0.65 Cr	0.10 Zr	/	/	/

Fracture toughness tests were performed on an MTS closed-loop servohydraulic test frame with the test furnace system (Model FR210), which allow elevated temperature fracture testing in vacuum. The nominal oxygen partial pressure was 2.57×10^{-10} Torr and the nominal water partial pressure was 1.23×10^{-9} Torr. Tungsten mesh heating element and molybdenum heat shields for operation to 1700°C in vacuum provide the usable work zone of 89mm in diameter and 127mm in height. Specimen temperatures were monitored and controlled by two Type K thermocouples attached to the specimen surface. Extensometry was achieved with a capacitive displacement device (Capacitec, Model 3201-SP amplifier and Model HPT-150 probe) which produces a voltage proportional to the gap spacing between the probe and the grounded plate. MTS 0.2" extensometer was used to calibrate the Capacitec probe at room temperature for each alloy. Fracture toughness tests over three temperatures, RT, 200, and 300°C, were conducted with notched tensile specimens and four-point bending bar specimens. Room temperature tests were performed in air, and high temperature tests were performed in vacuum. The heating rate was approximately 3.5°C/min for the elevated temperature tests. After reaching the desired temperature, the specimen was held in vacuum at temperature for approximately 0.5 hour to stabilize the temperature before loading. All fracture toughness tests were controlled with specialized LABVIEW software. For both notched tensile fracture tests and four-point bend tests, the same strain rates were chosen for each alloy considering the strain rate sensitivity of three copper alloys^[1]. The geometry of notched tensile specimens and four-point bending specimens is shown in figure 1. The notched tensile specimens were oriented in the L-S orientation with the notches perpendicular to the rolling direction. These specimens could not be fatigue-precracked because of relatively small diameter of notched section. A cross-head speed of 0.006 mm/sec was chosen consistent with ASTM E399. This cross-head speed corresponds to the strain rate of order of 10^{-4} s^{-1} , which is typically used in static fracture toughness tests. The four-point bend specimens were oriented in the L-S orientation

also with the notches perpendicular to the rolling direction. Dimensions of the as-received materials and the limitation of the vacuum chamber size prevent the use of ASTM standard size specimens. Efforts were made to satisfy ASTM standard in testing practice as closely as possible. The fatigue precracking from the notches was performed at room temperature in air prior to testing. Cyclical loading with the ratio of minimum to maximum load of 0.1 was chosen for cycles between 10^5 and 10^6 depending on the alloy. Sine waveform was used with the frequency of 3 Hz. In order to monitor the crack growth with microscope, the specimens were polished with 6 micron diamond polish before precracking. The nominal crack length (total length of the notch plus the fatigue crack) was about 0.3 to 0.4 of width. According to ASTM E399, the crosshead speed for fracture testing was chosen as 0.013mm/sec. The crack length measurements were confirmed with traveling microscopes.

A Perkin Elmer Phi 660 Auger microprobe was used to examine the fracture surface chemistry of the notched tensile specimens. To minimize oxidation of the fracture surfaces, failed specimens were unloaded and cut into Auger specimens in about half an hour. They were then kept under vacuum. Fractographic observations were made with a Hitachi S-800 SEM operated at 10 kV. Typical fracture surfaces are examined to identify the features relating to the fracture micromechanisms. Optical microscopy was used to examine the macroscopic characteristics of plastic zones and fracture surfaces of the specimens.

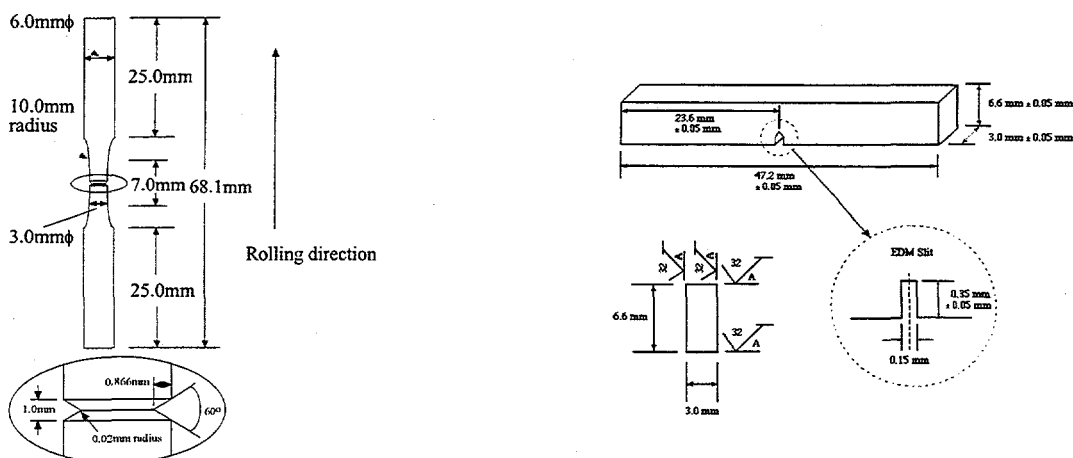


Figure 1. Geometry and size of notched tensile specimen and four-point bending specimen

3. Results

3.1 Fracture behavior of copper alloys

The plastic deformation and fracture behavior were found to be quite different among three copper alloys. Figure 2 shows load-displacement curves of notched tensile specimens for the three copper alloys at each of three test temperatures. Displacements were converted from Capacitec™ extension data by the calibration of extensometer at room temperature. GlidCop™ CuAl25 shows significant plastic deformation over three temperatures. The fracture loads decrease as temperature increases. Elbrodur CuCrZr shows larger plastic deformation compared with GlidCop™ CuAl25. Hycon 3HP CuNiBe shows relatively brittle behavior at all three temperatures compared with GlidCop™ CuAl25 and Elbrodur CuCrZr. Moreover, as temperature increases, brittle fracture in CuNiBe alloy is more evident, and the fracture loads decrease significantly. In order to compare the fracture behavior of each

copper alloy, fracture energy was obtained by integrating the area under each load-displacement curve. Figure 3 shows fracture energy versus temperatures of notched tensile specimens for three copper alloys. Fracture energy of GlidCop™ CuAl25 and Hycon 3HP CuNiBe decreases rapidly as the test temperature increases. For Elbrodur CuCrZr, the fracture energy does not show much change at 200°C, but decrease at 300°C. The fracture energy was also quite different at each test temperature depending on the material. Comparing these three alloys, fracture energy of CuCrZr is highest, and fracture energy of CuNiBe is lowest over the three temperatures. Figure 4 shows comparison of fracture energy with fracture toughness in the range of temperature 20°C to 300°C. The fracture toughness data were reported by D. J. Alexander [4]. All of these three copper alloys show similar trends of fracture energy decreases to fracture toughness decreases with increasing temperature. This comparison suggests that the relative fracture behavior of these copper alloys can be evaluated by simple tension tests. This is very useful for study of fracture micromechanism analysis where the exact values of fracture toughness are not critical.

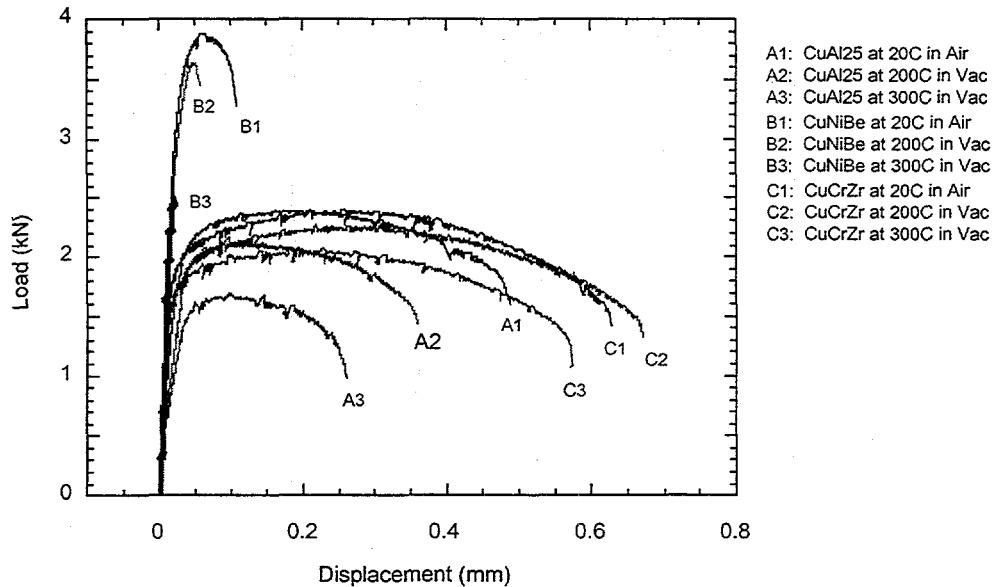


Figure 2. Load vs. displacement of notched tensile specimens for three copper alloys

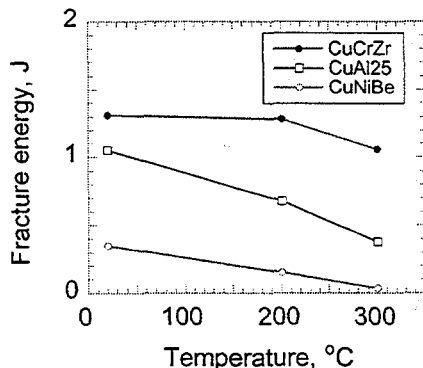


Figure 3. Fracture energy versus temperature of notched tensile specimens for three copper alloys

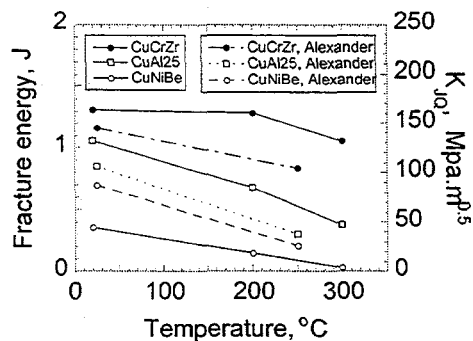


Figure 4. Comparison of fracture energy with fracture toughness of notched tensile specimens for three copper alloys

3.2 Fracture surface analysis

The fracture surfaces of the notched tensile specimens were examined by SEM to identify the significant features relating to the fracture performance. A macroscopic comparison of room temperature and 200°C conditions on the fracture surfaces for CuAl25 indicates that the fracture surfaces of both specimens are reasonably flat. A close examination of failure surfaces shows that at 20 and 200°C, both specimens have a large amount of plasticity-induced microvoid formation, which can be seen in figure 5. Figure 6 shows the failure surfaces of CuNiBe tested at 20, 200, and 300°C. All specimens show mixed modes of transgranular fracture and intergranular fracture; the percentage of intergranular fracture increases as the test temperature increases. This percentage increase of intergranular fracture corresponds to the fracture energy change at the different temperatures. Fractographic examinations of CuCrZr alloy over three temperatures are shown in figure 7. Microvoid coalescence is the main fracture mechanism for CuCrZr alloy at all test temperatures. The depth and width of the observed dimples are very similar at all three temperatures. Compared to CuAl25, the dimple size of CuCrZr alloy is larger than that of CuAl25 alloy. At higher magnification, cracking second-phase particles are visible inside dimples.

The fracture surface chemistry was thoroughly analyzed by Auger Electron Spectroscopy. Auger spectra were taken from fracture surfaces of CuAl25 tested at room temperature and 200°C temperature. Significant oxygen, carbon and chlorine are presented on fracture surfaces. Chlorine was probably from lab water vaporization. No aluminum was observed. Chemical mapping of chlorine and copper on CuAl25 failure surface at 200°C does not provide much information. Auger spectra were also taken on fracture surfaces on CuNiBe at 300°C temperature. Both area-analysis and point-analysis show significant amount of oxygen, carbon, silicon and chlorine. No beryllium segregation near grain boundaries can be detected. Composition-depth profiles on and adjacent to grain boundaries on the fracture surface of CuNiBe at 300°C do not show much difference in the distribution of beryllium and nickel. Auger analysis on the fracture surfaces of CuCrZr alloy tested at 300°C shows similar results. These results are clouded by the formation of oxides at the free fracture surfaces. Continuing work aimed at addressing this problem.

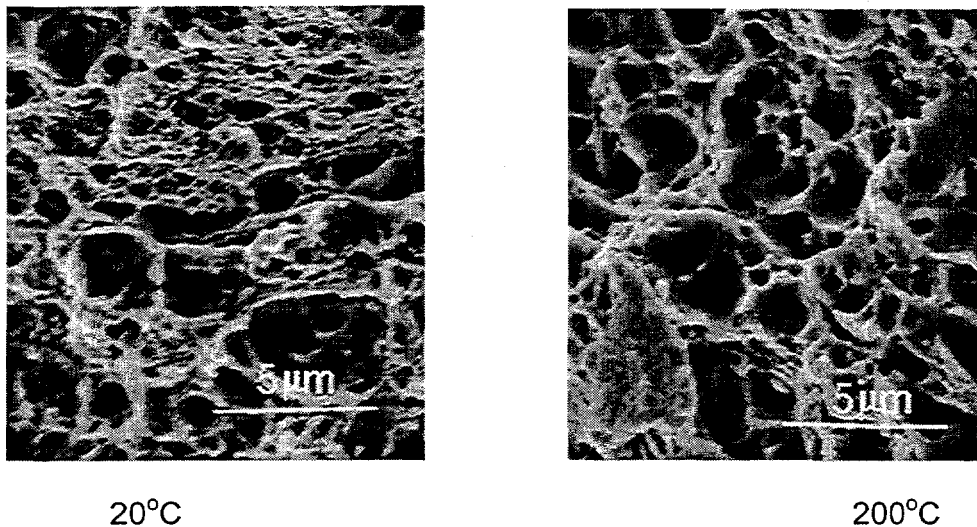


Figure 5. SEM fractographs of the fracture surfaces of notched tensile specimens for CuAl25

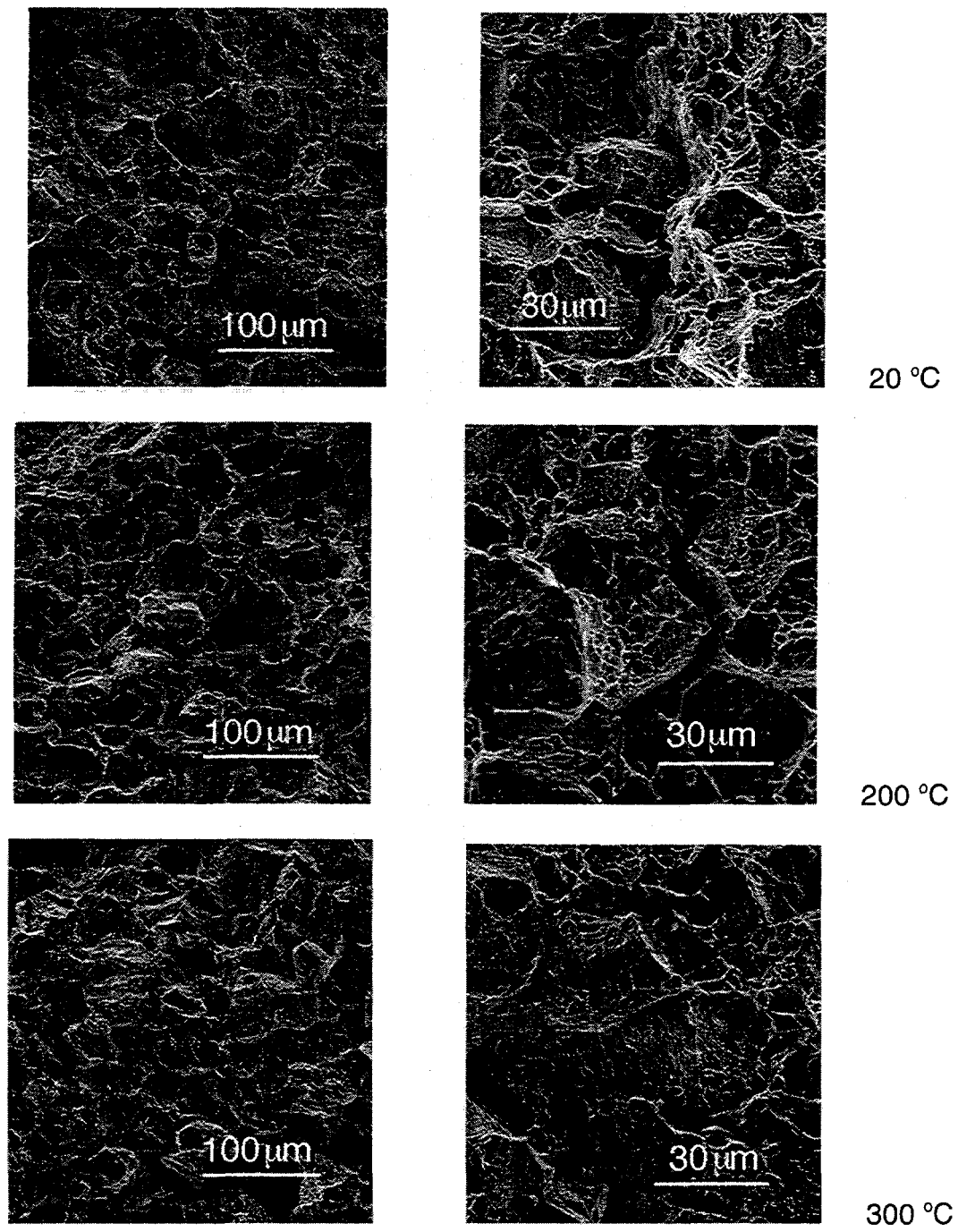


Figure 6. SEM fractographs of the fracture surfaces of notched tensile specimens for CuNiBe

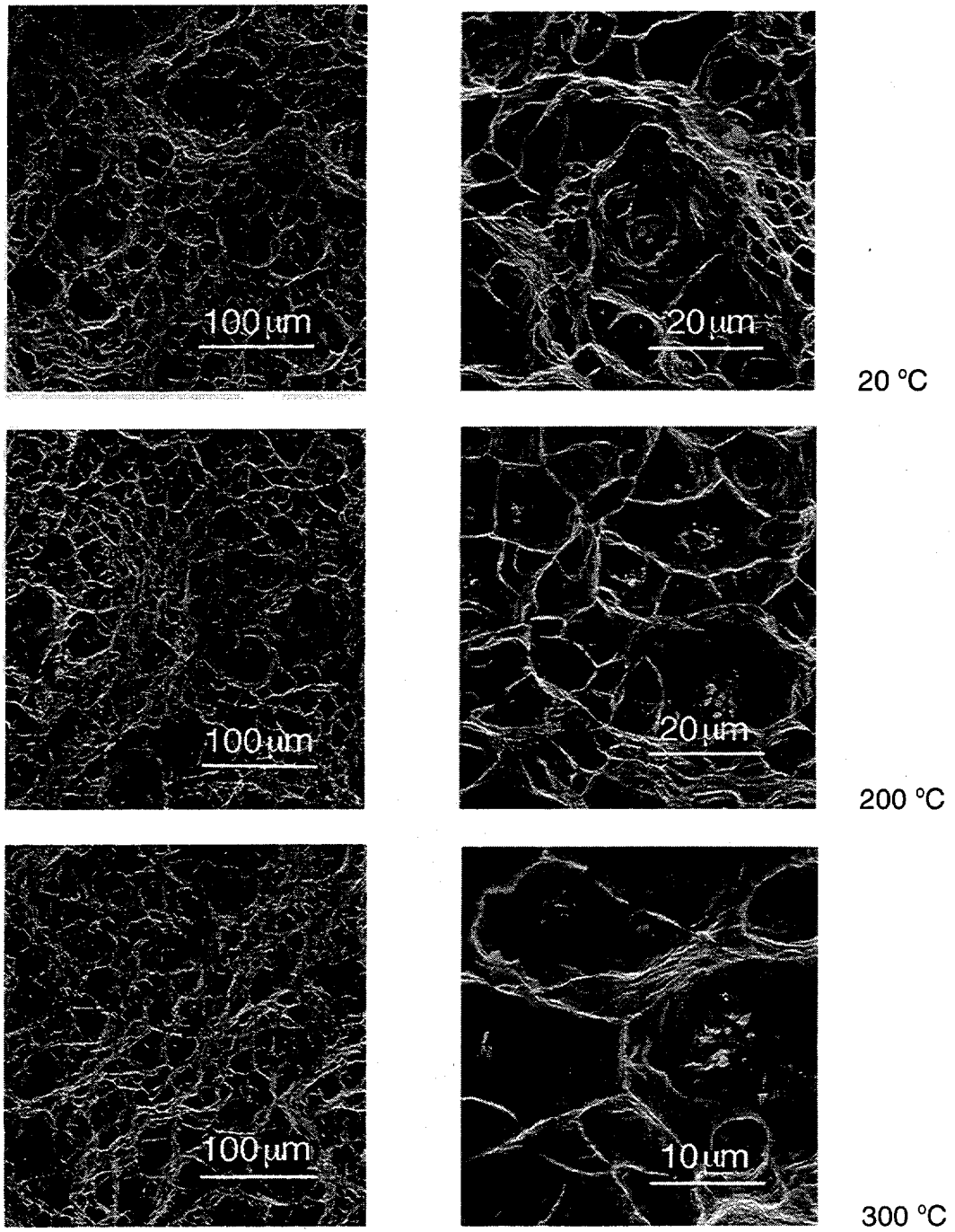


Figure 7. SEM fractographs of the fracture surfaces of notched tensile specimens for CuCrZr

3.3 Fracture behavior analysis on four-point bending specimens

The precracked four-point bend specimens were used for fracture toughness tests to determine temperature effects. Subsize specimens were intended for J-integral fracture toughness tests. Limitation in the specimen dimension and the testing machine prevented valid J-integral fracture tests. Measurements of fracture toughness, K_Q , succeeded on CuNiBe alloy, but failed on CuAl25 and CuCrZr alloys due to rather ductile behavior in these cases. The K_Q measurements for CuNiBe alloy are shown in figure 8. The plot shows that fracture toughness decreases rapidly as the temperature increases. Compared to the data from Alexander [4], significant differences exist for the room temperature value (figure 9), most likely due to constraint considerations at the most ductile condition.

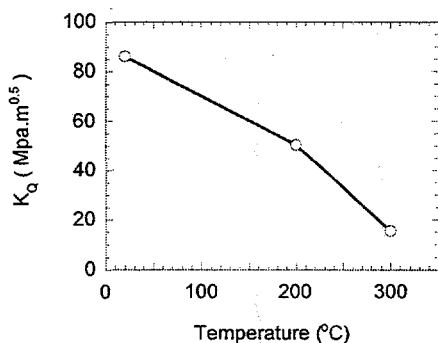


Figure 8. Fracture toughness vs. temperature of four-point bending tests for CuNiBe

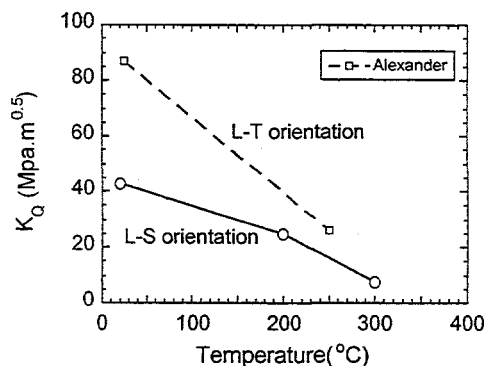


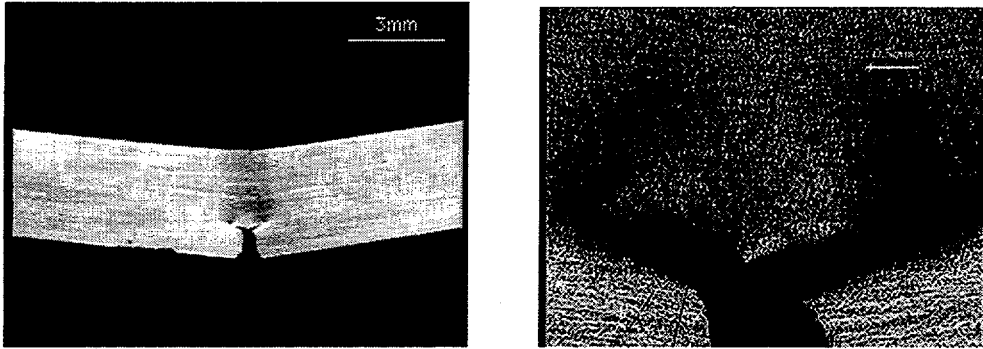
Figure 9. Comparison of fracture toughness of CuNiBe with data after Alexander

Although no valid fracture toughness values were obtained on CuAl25 and CuCrZr alloys, the macroscopic observations of failed specimens of three copper alloys by optical microscopy show quite different fracture features, see figure 10. The CuCrZr alloy shows significant plastic zones at both room temperature and 300°C. There is no visible crack growth. CuAl25 alloy shows similar plastic zone characteristic to the CuCrZr alloy at room temperature test. However, the fracture features are markedly different at 300°C.

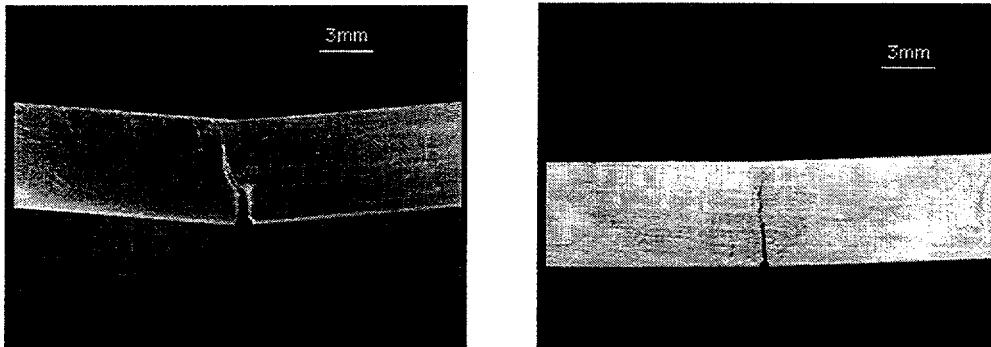
It is interesting to note that not only a relatively large plastic zone is formed around the initial crack, but also two cracks extend in opposite directions perpendicular to the initial crack direction. This indicates the strong preference for crack growth along the rolling directions instead of the initial crack direction. The CuNiBe specimen shows an initial shear crack growth mode at room temperature. At 300°C, the crack extends straight along the initial crack direction.

Discussion

The main purpose of this study was to investigate the effect of temperature on the fracture behavior and the fracture mechanisms of copper alloys at high temperatures. While it is most convenient to evaluate the fracture toughness by standard procedures, the limitation in the dimension of the material and other factors necessitates the development of a non-standard method, mostly the design of a non-standard specimen geometry. Notch tension testing is an attractive method for obtaining a fast inexpensive estimate of a material's toughness with reasonable accuracy. Fracture energy of notched tensile specimens for copper alloys gives the relative accurate evaluation of fracture toughness of materials. Notch tension testing provides a useful estimation of fracture behavior in case that focus is



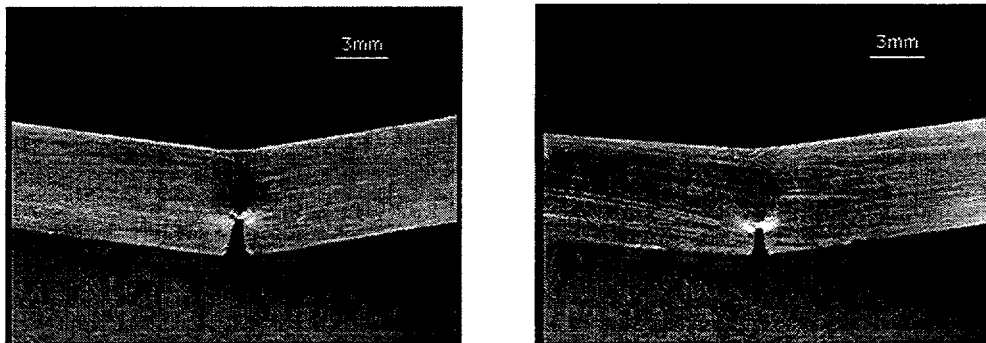
(a) Fracture feature of four-point bending specimen for CuAl25 at 300°C test at low magnification and high magnification



20°C

300°C

(b) Fracture features of four-point bending specimen for CuNiBe at 20 and 300°C tests



20°C

300°C

(c) Fracture features of four-point bending specimen for CuCrZr at 20 and at 300°C tests

Figure 10. Fracture features of four-point bending specimens of three copper alloys

on the fracture mechanism analysis. Due to the small diameter of notched section, it was not possible to fatigue-precrack the notched tensile specimens. This might be one of reasons that fracture testing at elevated temperature results in transgranular fracture mode instead of expected intergranular fracture mode. Most of the fracture energy was likely consumed in the crack initiation processes.

All elevated temperature fracture tests were performed in vacuum. Both notched tensile fracture tests and four-point bending fracture tests indicate that the fracture behaviors of three copper alloys degraded as temperature increased, however, CuCrZr shows less degradation compared to CuAl25 and CuNiBe alloys. The literature suggests that environmental effects could be a factor responsible for the poor fracture toughness of copper alloys [4]. This study provides the evidence that an environmental effect can not be the predominant cause of poor fracture toughness.

The SEM fracture surface morphology reveals that CuNiBe shows mixed intergranular and transgranular fracture modes. This intergranular fracture can result from a number of processes. Microvoid nucleation and coalescence at inclusions or second-phase particles located along grain boundaries, grain boundary crack and cavity formation associated with elevated temperature stress rupture, decohesion between contiguous grains due to the presence of brittle elements at grain boundaries, and insufficient number of independent slip systems to accommodate plastic deformation between contiguous grains could be the cause of grain boundary separation [3]. Be is believed to be the most critical element concerning intergranular fracture of CuNiBe. For CuCrZr alloy, tests at all three temperatures show similar microvoid coalescence fracture mechanism. Second-phase particle cracking provided the nucleation sites of microvoids. Compared to CuNiBe and CuCrZr alloys, it is more complicated to identify the fracture mechanism of CuAl25 alloy. Both notched tensile tests and four-point bending fracture tests show that fracture behavior degrades relatively rapidly with increasing temperature.

ACKNOWLEDGEMENTS

This work was supported by the Associated Western Universities (AWU) through a grant from the Pacific Northwest National Laboratory (PNNL) under the US DOE Fusion Materials Program, as well as by OMG Americas, Inc. and Brush Wellman, Inc.. We would like to express our appreciation to D. J. Edwards, PNNL, and the US DOE Fusion Materials Program for supplying the GlidCop and Hycon materials, produced by OMG Americas, Inc. and Brush Wellman, Inc. respectively. We would also like to thank S. J. Zinkle, ORNL, for supplying the CuCrZr alloy. The Advanced Materials Testing and Evaluation Laboratory (AMTEL), UIUC and the Center for Microanalysis of Materials in Seitz Materials Research Laboratory, UIUC provided the mechanical testing facilities and microanalysis facilities.

REFERENCES

1. S. J. Zinkle and W. S. Eatherly, Fusion materials Semiannual progress Report, DOE/ER-0313/21 (1996) 165
2. K. D. Leedy, J. F. Stubbins, D. J. Edwards, and R. R. Solomon, Fusion Materials Semiannual progress Report, DOE/ER-0313/22 (1997) 149.
3. K. D. Leedy, Ph.D. Thesis, University of Illinois at Urbana-Champaign, 1997
4. D. J. Alexander, S. J. Zinkle, and A. F. Rowcliffe, Fusion Materials Semiannual Progress Report, DOE/ER-0313/21 (1996) 175.
5. R. W. Hertzberg, Deformation and Fracture Mechanics of Engineering Materials, 1983